

Spatio-temporal variability of zooplankton standing stock in
eastern Arabian Sea inferred from ADCP backscatter
measurements

Ranjan Kumar Sahu, P. Amol, D.V. Desai, S.G. Aparna, D. Shankar

July 2, 2024

Abstract

We use acoustic Doppler current profiler (ADCP) backscatter measurements to map the spatio-temporal variation of zooplankton standing stock in the eastern Arabian Sea (EAS). The ADCP moorings were deployed at seven locations on the continental slope off the west coast of India; we use data from October 2017 to December 2023. The 153.3 kHz ADCP uses backscatter from sediments or organisms such as copepods, ctenophores, salps and amphipods greater than 1 cm to calculate current profile. The backscatter is obtained from echo intensity using RSSI conversion factor after doing necessary calibrations. The conversion from backscatter to biomass is based on volumetric zooplankton sampling at the respective locations. Analysis of the data over 24 – 120 m shows that the backscatter and zooplankton biomass decrease from the upper ocean (215 m g^{-3} biomass contour) to the lower depths. Changes are observed in the seasonal variation of the monthly

¹² climatology of zooplankton standing stock (integral of the biomass over 24 – 120 m water column)
¹³ as we move to poleward along the slope in EAS. The range of variation of standing stock is lowest
¹⁴ at Kanyakumari, followed by Okha, which lie at the southern and northern boundary of the EAS,
¹⁵ respectively. Complementary variables are used to explain the processes leading to growth or decay
¹⁶ of zooplankton biomass.

₁₇ **1 Introduction**

₁₈ **1.1 Background**

₁₉ Zooplankton plays a vital role in food web of pelagic ecosystem by enabling the hierarchical trans-
₂₀ port of organic matter from primary producers to higher trophic levels impacting the fish population
₂₁ and the carbon pump of the deep ocean [Ohman and Hirche, 2001, Le Qu et al., 2016]. They are
₂₂ presumably the largest migrating organisms in terms of biomass [Hays, 2003] which occurs in diel
₂₃ vertical migration (DVM). Zooplanktons depend not only on phytoplankton but other environ-
₂₄ mental parameters (e.g. Mixed layer depth, insolation, Oxygen, thermocline, nutrient availability,
₂₅ chlorophyll concentration and daily primary production). The biological productivity of the ocean
₂₆ is essentially connected with physics and chemistry [Subrahmanyam, 1959, Ryther et al., 1966,
₂₇ Qasim, 1977, Nair, 1970, Banse, 1995, McCreary et al., 2009, Vijith et al., 2016, Amol et al., 2020].
₂₈ The dynamic ocean results in varying physico-chemical properties, leading to bloom and growth of
₂₉ planktons in favourable conditions. The changes are strongly influenced by the seasonal cycle in
₃₀ the North Indian Ocean (NIO; north of 5 °N of Indian Ocean). The eastern boundary of Arabian
₃₁ Sea contains the West India Coastal Current (WICC; [Patil et al., 1964, Ramamirtham and Murty,
₃₂ 1965, Banse, 1968, Shetye et al., 1991, McCreary Jr et al., 1993, Shankar and Shetye, 1997, Shetye
₃₃ and Gouveia, 1998, Maheswaran et al., 2000, Amol et al., 2014, Chaudhuri et al., 2020, 2021])
₃₄ which reverses seasonally, flowing poleward (equatorward) during November to February (June to
₃₅ September).
₃₆ The direct consequence of this reversal is the seasonal cycle of thermocline, oxycline and thick-
₃₇ ness of mixed Layer Depth (MLD) induced by upwelling favourable conditions in summer and down-
₃₈ welling favourable conditions in winter in eastern Arabian Sea (EAS). Further, the phytoplankton

39 biomass and chlorophyll concentration changes with the season [Subrahmanyam and Sarma, 1960,
40 Banse, 1968, Lévy et al., 2007, Vijith et al., 2016]. Upwelling in summer monsoon leads to maxi-
41 mum chlorophyll growth in the entire EAS [Banse, 1968, Banse and English, 2000, McCreary et al.,
42 2009, Hood et al., 2017]. During winter monsoon, the convective mixing induced winter mixed layer
43 [Shetye et al., 1992, Madhupratap et al., 1996b, Lévy et al., 2007, Vijith et al., 2016, Shankar et al.,
44 2016, Keerthi et al., 2017] results in winter chlorophyll peak in northern EAS (NEAS) while the
45 downwelling Rossby waves modulate chlorophyll along the southern EAS (SEAS) albeit limited to
46 coast and islands [Amol et al., 2020]. (For a detailed description on EAS division, please refer figure
47 1 of [Shankar et al., 2019].

48 The zooplankton grazing peak is instantaneous with no time delay from peak phytoplankton
49 production [Li et al., 2000], but its population growth lags [Rehim and Imran, 2012, Almén and
50 Tamelander, 2020] depending on its gestation period and other limiting aspects. While some studies
51 suggest that the peak timing of zooplankton may not change in parallel with phytoplankton blooms
52 [Winder and Schindler, 2004], others indicate that lag exists between primary production and the
53 transfer of energy to higher trophic levels [Brock and McClain, 1992, Brock et al., 1991]. A recent
54 work [Aparna et al., 2022] had shown that peak zooplankton population may never occur even
55 with a bloom in phytoplankton such as in SEAS, leading to the collapse of ecological models and
56 succeeding food webs of higher trophic levels.

57 The conventional zooplankton measurements, where only few snapshot/s of the event is cap-
58 tured gives an incoherent or incomplete understanding in terms of spatio-temporal variation of
59 zooplankton [Ramamurthy, 1965, Piontkovski et al., 1995, Madhupratap et al., 1992, 1996a, Wish-
60 ner et al., 1998] as much information is revealed by later studies [Jyothibabu et al., 2010, Vijith
61 et al., 2016, Shankar et al., 2019, Aparna et al., 2022] using high resolution data. Calibrated acous-

tic instruments such as Acoustic Doppler Current Profiler (ADCP) along with relevant data can be utilised to understand small scale variability [Nair et al., 1999, Edvardsen et al., 2003, Smith and Madhupratap, 2005, Smeti et al., 2015, Kang et al., 2024], the complex interplay between the physico-chemical parameters and ecosystem [Jiang et al., 2007, Potiris et al., 2018, Shankar et al., 2019, Aparna et al., 2022, Nie et al., 2023], the zooplankton migration [Inoue et al., 2016, Ursella et al., 2018, 2021] and their seasonal to annual variation [Jiang et al., 2007, Hobbs et al., 2021, Liu et al., 2022, Aparna et al., 2022].

69 1.2 ADCP backscatter and zooplankton biomass

70 At present, there are two types of acoustic samplers: non-calibrated single frequency acoustic profiler such as ADCP or calibrated multi and mono frequency acoustic profilers such as zooplankton acoustic profiler (ZAP) and Tracor acoustic profiling system(TAPS). The use of acoustics as a proxy for zooplankton biomass estimation can be traced to [Pieper, 1971, Sameoto and Paulowich, 1977] and earlier studies which used echograms to approximate the large-scale horizontal extents [Barraclough et al., 1969], and small scale vertical extent [McNaught, 1968]. The relationship between backscatter and the abundance and size of zooplankton was described by [Greenlaw, 1979] wherein it was pointed out that single frequency backscatter can be used to estimate abundance if mean zooplankton size is known. This paved the way for use of single frequency acoustic profiler. A drastic increase in study temporal and spatial variation of zooplankton biomass using backscatter-proxy came in 1990s by introduction of high frequency echo sounders, with studies [Flagg and Smith, 1989, Wiebe et al., 1990, Batchelder et al., 1995, Greene et al., 1998, Rippeth and Simpson, 1998] methodically showing acoustic backscatter estimated zooplankton biomass in various shelf and slope locations around North Atlantic, North pacific location. The foundation for further research that

84 investigated the potential of acoustic backscatter from ADCPs and multi frequency echo sounders
85 in assessing zooplankton biomass and comprehending zooplankton dynamics in diverse maritime
86 habitats was established by these initial explorative experiments.

87 Acoustic backscatter and zooplankton biomass have been better understood as a result of tech-
88 nological and methodological developments over time. Net sampling augmented ADCP backscatter
89 have been used to study DVM and the spatial and temporal variability of zooplankton biomass by
90 [Cisewski et al., 2010, Smeti et al., 2015, Guerra et al., 2019] in different marine regions, such as the
91 Southwestern Pacific, the Lazarev Sea in Antarctica and the Corsica Channel in the north-western
92 Mediterranean Sea. The zooplankton biomass variation in the Arabian sea has been studied during
93 JGOFS programme in 1990s [Herring et al., 1998, Nair et al., 1999, Fielding et al., 2004, Smith and
94 Madhupratap, 2005]. However, their studies were limited to the cruise duration as vessel mounted
95 ADCPs were predominantly used; hence long-term data was sparsely produced. The first such
96 study to fully exploit the immense potential of ADCPs in EAS was carried out by [Aparna et al.,
97 2022] using ADCP moorings deployed on continental slopes off the Indian west coasts [Amol et al.,
98 2014, Chaudhuri et al., 2020].

99 1.3 Objective and scope of the manuscript

100 A network of ADCPs has been installed off the continental slope and shelf on the west coast of
101 India. This ADCPs have enabled a rigorous view of intraseasonal to seasonal scale variability [Amol
102 et al., 2014, Chaudhuri et al., 2020]. Initially a network of 4 ADCPs (off Mumbai, Goa, Kollam and
103 Kanyakumari) on continental slope, it has been extended to include 3 more moorings (off Okha from
104 2018, Jaigarh and Udupi from 2017). In the recent study [Aparna et al., 2022] have used ADCP
105 moorings off Mumbai, Goa and Kollam to explain the temporal variability of zooplankton biomass.

106 The study showed that the zooplankton peaks (and troughs) is not only non-uniform in latitude but
107 also heavily influenced by the oxygen minimum zone, MLD and the seasonal upwelling/downwelling
108 conditions. Stark contrast in the phytoplankton bloom and subsequence growth of zooplankton or
109 the lack thereof was observed in the EAS regimes.

110 We build upon the existing work by extending to include the newly incorporated ADCPs so as to
111 have a better understanding in the latitudinal variation of zooplankton biomass in EAS. The paper
112 is organized as follows; datasets and methods employed are described in detail in Section 2. Section
113 3 describes the observed climatology of zooplankton biomass and standing stock. A comparison is
114 drawn to the results of previous studies at the overlapping mooring sites. Further, the seasonal cycle
115 of zooplankton biomass and standing stock is discussed. The role of mixed layer depth, net primary
116 production, sea surface temperature, wind forcing and circulation in determining the biomass is
117 discussed in results section 4, with conclusion in section 5.

118 2 Data and methods

119 The backscatter data from ADCP and the zooplankton samples collected from the periphery of
120 mooring is described in this section. The methodology followed in processing ADCP data and
121 estimation of backscatter and subsequently the zooplankton biomass is discussed. The backscatter
122 derived from the echo intensity of the seven ADCP mooring deployed on the continental slope off
123 the Indian west coast is the primary data we have use in this manuscript. The moorings details are
124 summarised in [Table 1](#). In situ biomass data from volumetric zooplankton samples are used to val-
125 idate and correlate with backscatter. The chlorophyll data is obtained from marine.copernicus.eu.
126 In addition, we have used the monthly climatology of temperature and salinity [[Chatterjee et al.,](#)
127 [2012](#)] and the net primary productivity from MODIS (Moderate Resolution Imaging Spectrora-

¹²⁸ diometer) and VIIRS (Visible Infrared Imaging Radiometer Suite) from global NPP estimates
¹²⁹ (<http://sites.science.oregonstate.edu/ocean.productivity>).

¹³⁰ 2.1 ADCP data and Backscatter estimation

¹³¹ The ADCPs were deployed on the continental slope off the Indian west coast (Fig. 1). Initially a
¹³² set of three ADCPs, it was gradually extended to four more sites to cover the entire EAS basin
¹³³ from Okha (22.26°N) in north to Kanyakumari (6.96 °N) in south. The other two ADCPs are
¹³⁴ Jaigarh at central EAS (CEAS) and Udupi in the transition zone between CEAS & SEAS. The
¹³⁵ extended moorings were deployed in October 2017, except for Kanyakumari which was deployed
¹³⁶ earlier as well but it wasn't included in earlier backscatter study. The moorings are serviced on
¹³⁷ yearly basis usually during October-November or in winter monsoon months. The ADCPs are of
¹³⁸ RD Instruments make, upward-looking and operate at 153.3 kHz. While utmost care is taken to
¹³⁹ position the instrument at ~ 200 m depth, yet for some deployments it's shallow or deeper owing
¹⁴⁰ to drift caused by floater buoyancy - anchor weight balance. Data was collected at hourly interval
¹⁴¹ and the bin size was set to 4 m. The echoes at surface to 10 % range (20 m) means the data at
¹⁴² these is rendered useless and is discarded from further use.

¹⁴³ The procedure followed in processing of the ADCP data are described in [Amol et al., 2014]
¹⁴⁴ and [Mukherjee et al., 2014]. An addition to their methodology was to do depth correction to ac-
¹⁴⁵ commodate the vertical movement of ADCP buoys [Chaudhuri et al., 2020, Mukhopadhyay et al.,
¹⁴⁶ 2020] using data from pressure sensor mounted on the instrument. We have followed the method-
¹⁴⁷ ology laid down in [Aparna et al., 2022] to derive the backscatter time series from ADCP echo
¹⁴⁸ intensity data which is discussed later paragraph. The gaps are filled using the grafting method of
¹⁴⁹ [Mukhopadhyay et al., 2020] once the zooplankton biomass time series is constructed.

150 The primary objective of ADCP usage is to obtain vertical current profile at a point location. It
151 is achieved by using the echo intensity received at the ADCP transducer. The instrument sensors
152 doesn't directly give backscatter, as echo intensity is range independent. Range correction has to
153 be performed before echo intensity (E) is converted to Backscatter (B). Received signal strength
154 indicator (RSSI), also called the conversion factor (K_c) which is specific to a sensor is used along with
155 the corresponding reference echo intensity (E_r). It's important to state that for the same device K_c
156 remains unchanged while E_r varies over each subsequent deployment. The backscattering strength
157 (in dB) is given by [Mullison, 2017]:

$$158 \quad B = [C - L_{DBM} - P_{DBW}] + 2\alpha R + 10\log_{10}[(T_{TD} + 273.16)R^2] + 10\log_{10}[10^{K_c(E-E_r)/10} - 1]$$

159 where C is an empirical constant, L_{DBM} is $10\log_{10}L$ where L is the transmit pulse length in
160 meters, P_{DBW} is $10\log_{10}P$ (P is transmitted power in watts), α is the sound absorption coefficient
161 of water (in $dB m^{-1}$), T_{TD} is the temperature (in ${}^\circ C$) at the depth of positioned instrument, R
162 is the slant range (in meters) from transducer to the scatterers and E_r is the reference level of E
163 taken in real-time (unit counts). E_r in our case is taken from first (last) measured profile when the
164 instrument is in air before (after) deployment (retrieval). The backscattering strength is referenced
165 to $(4\pi m^{-1})$ [Deines, 1999, Mullison, 2017]. Aparna et al. [2022] has discussed the relevance of each
166 of the term to the total backscattering strength. Our analysis also suggests that the α does not
167 affect the final results.

168 2.2 Zooplankton data and estimation of biomass

169 The zooplankton samples were collected in the vicinity (~ 10 km) of ADCP mooring site twice; once
170 prior retrieval and again post deployment of moorings so that there is overlap in the ADCP time
171 instance and in situ zooplankton samples. The sampling is done at the mooring location during

¹⁷² servicing cruises on board RV Sindhu Sankalp and RV Sindhu Sadhana (Table 2). Multi-plankton
¹⁷³ net (MPN) (100 μm mesh size, 0.5 m^2 mouth area) was used to get samples in the pre-determined
¹⁷⁴ depth ranges; water volume filtered was calculated by the product of sampling depth range and the
¹⁷⁵ mouth area of net. The depth range and timing of sample collection was different throughout the
¹⁷⁶ MPN hauls (refer [Table 2](#)). From 2020 onward, the depth-range was standardized to the bins of 0
¹⁷⁷ - 25, 25 - 50, 50 - 75, 75 - 100, 100 - 150 (units are in meters). The collected zooplankton samples
¹⁷⁸ were then preserved in 5 % formaldehyde solution until it's transferred to laboratory. To measure
¹⁷⁹ zooplankton wet weight accurately, the gelatinous forms/salps were separated. [[Aparna et al.,](#)
¹⁸⁰ [2022](#)] had reported the calanoid copepods, cyclopoid copepods, Poecilostomatoida, Harpacticoida,
¹⁸¹ appendicularians, euphausids, ostracods, and chaetognaths as the major groups of zooplanktons
¹⁸² contributing to the biomass of net samples from the mooring sites. The backscatter obtained earlier
¹⁸³ is averaged in vertical corresponding to the specific MPN hauls for each site. The backscatter is
¹⁸⁴ linear regressed with respective biomass to establish their relationship, which has been demonstrated
¹⁸⁵ in numerous previous studies [[Flagg and Smith, 1989](#), [Heywood et al., 1991](#), [Jiang et al., 2007](#),
¹⁸⁶ [Aparna et al., 2022](#)].

¹⁸⁷ We calculated the regression equation to be $y = 0.0203 x + 4.01$ and, which is well within the
¹⁸⁸ error range of the regression equation of [[Aparna et al., 2022](#)], $y = (0.02 \pm 0.004) x + (4.14 \pm 0.36)$
¹⁸⁹ with a correlation of 0.53 ([Fig. 2](#)). The correlation value in our case is 0.54; the minor difference is
¹⁹⁰ due to higher number of data points (159) in the present study.

¹⁹¹ **2.3 Biomass time series and estimation of standing stock**

¹⁹² The zooplankton biomass time series ([Fig. 3](#)) is created from the above derived linear relationship:
¹⁹³ $\log_{10}(\text{biomass}) = m * \text{Backscatter} + k$, where m is slope and k is intercept. The time series shows

194 the pattern of diel vertical migration (DVM) at all the mooring sites during dawn (\sim 0600-0700
195 hours) and dusk (\sim 1800-1900 hours). It is evident in earlier studies using backscatter [Ashjian
196 et al., 2002, Smith and Madhupratap, 2005, Inoue et al., 2016, Ursella et al., 2018] and in situ
197 zooplankton data [Padmavati et al., 1998]. The implication of DVM is a higher biomass at surface
198 during the night as zooplankton feeds and a lower biomass at daytime as they descend to subsurface
199 depths. The overall biomass over the time period of a day may vary but the DVM doesn't affect
200 the seasonal variation as shown by ([Jiang et al., 2007, Aparna et al., 2022]). Since our goal is to
201 study the seasonal variation, delineating the daily biomass is sufficient. The biomass time series
202 and seasonal cycle is discussed in subsection 4.1.

203 The standing stock is determined by taking the depth integral of biomass over the water column.
204 To maintain the consistency of standing stock estimation, only those deployments that doesn't lack
205 data at any depth in the entire range of 24 - 120 m are considered for analysis. The lack of data in
206 the above mentioned depth range is due to deviation in positioning of ADCP sensor in the water
207 column. A swift alteration in bathymetry along the continental slope implies that the mooring
208 might anchor at a different depth than planned, hence a change in the predicted position of ADCP.
209 This leads to gap in data at few mooring sites for some year. For example, for the northern-most
210 mooring at Okha, data is not available for the entire upper 120 m depth for the second deployment.
211 Also at Jaigarh, where the surface to \sim 60m data (in 3rd deployment) and Kollam, where 80 m
212 and below (in 4th deployment) is unavailable and hence discarded from standing stock estimation.
213 There are few deployments where no data or bad data was recorded e.g, at Udupi (4th deployment)
214 and Kanyakumari (6th deployment). The seasonal cycle of standing stock for 24 - 120 m available
215 data is explored in subsection 4.1.

216 **2.4 Mixed-layer depth, temperature and oxygen**

217 As we are using a 153.3 kHz ADCP moored at \sim 150 m, the top \sim 10% of data is unusable
218 because of surface echoes. MLD in EAS is of the order \sim 20 to 40 m during summer monsoon
219 [Shetye et al., 1990, Sreenivas et al., 2008] especially in the SEAS. Although it is possible to use
220 the near surface ADCP data after due noise correction; it is beyond the scope of present study.
221 The temperature data is used from [Chatterjee et al., 2012] which is a monthly climatology having
222 1° spatial resolution. Monthly climatology of oxygen data is obtained from World Ocean Atlas
223 2013 [García et al., 2014] which contains objectively analyzed 1° climatological fields of in situ
224 measurements.

225 **2.5 Chlorophyll and net primary productivity data**

226 Previous study based on ADCP data of EAS [Aparna et al., 2022] have used SeaWiFS based chloro-
227 phyll data for comparison with climatology of zooplankton standing stock (ZSS). The SeaWiFS was
228 at its end of service in 2010, hence we use new chlorophyll product. The present study has been
229 conducted using Global Ocean Colour, biogeochemical, L3 data obtained from the [E.U. Copernicus](#)
230 [Marine Service Information](#). The daily data is available at a spatial resolution of 4 km.

231 While chlorophyll is used to compare with the variation in climatology of zooplankton standing;
232 the growth efficiencies of zooplankton are directly linked to primary production levels, emphasizing
233 the interconnectedness between primary producers and consumers in marine food webs [?]. In
234 their study, [Aparna et al., 2022] has emphasized on the collapse of the predator-prey relationship
235 between zooplankton-phytoplankton using climatological data. We showcase their interdependency
236 or the lack thereof using net primary productivity models. Moderate Resolution Imaging Spectro-
237 radiometer (MODIS) based net primary productivity (NPP) data at a resolution of $0.16^{\circ} \times 0.16^{\circ}$

238 was obtained from Oregon State University. They have employed three different schemes to obtain
239 NPP from Chlorophyll concentration. Those are discussed below in brief. The first is Vertically
240 Generalized Production Model (VGPM). The NPP (a rate term) is to be derived from chlorophyll
241 (a standing stock) using chlorophyll-specific assimilation efficiency for carbon fixation. The single
242 biggest unknown in all models based on chlorophyll is how this rate term is described. VGPM
243 considers the primary productivity to be dependent on day length and maximum daily NPP within
244 a water column. The second is Carbon-based Productivity Model (CbPM) which NPP to phy-
245toplankton carbon biomass and growth rate. The third is Carbon, Absorption, and Fluorescence
246 Euphotic-resolving (CAFE) mode; first described by [Silsbe et al., 2016] takes various other factors
247 into NPP calculations. We explore these NPP models and try to explain the variation in ZSS.

248 3 Climatology of zooplankton biomass and standing stock

249 The previous study of zooplankton in EAS based on ADCP backscatter was consisting of three
250 sites: Mumbai in NEAS, Goa in CEAS and Kollam in SEAS. The extended mooring sites are at
251 Okha at NEAS, Jaigarh at CEAS, Udupi in the transition zone of CEAS & SEAS and Kanyakumari
252 at SEAS is the southern most location in our study area.

253 ADCP data from three mooring sites were analysed from 2012 to 2020 in [Aparna et al., 2022].
254 They have fine-tuned the methodology to obtain backscatter and estimated zooplankton biomass
255 from it using in situ volumetric zooplankton biomass data. A comparison is made in later para-
256 graphs, since the methodology remains same in the current study and new time series data is
257 available. The monthly climatology of biomass and ZSS is computed for all locations having valid
258 data in 24 - 120 m depth range ([Fig. 4](#)).

259 The high biomass regime in the upper ocean and low biomass regime in deeper depths is dif-

260 ferentiated using a biomass contour: 215 mg m^{-3} off Mumbai, Goa and Kollam; 200 mg m^{-3} off
261 Jaigarh and Udupi; 175 mg m^{-3} off Okha and Kanyakumari. For simplicity, this biomass contour
262 is abbreviated to be z215, z200 & z175 and its depth is denoted as D215, D200 & D175, respec-
263 tively. The choice of biomass contour isn't abrupt; firstly, it is carefully chosen to accommodate the
264 seasonal variation, as a shift to biomass contour lower than the z215 would be unviable as our data
265 is only till 140 m depth as in the case of Kollam. A higher biomass contour would lead to inferior
266 view of the seasonal cycle such as in the case of Kanyakumari and Okha where 215 mg m^{-3} biomass
267 contour is often low enough to reach $\sim 20 - 30$ m depths, hence z175 is chosen here. Secondly, it
268 allows us to link the seasonal variation of biomass to the physico-chemical properties.

269 The climatology of zooplankton biomass ([Fig. 4](#)) is discussed at locations northward starting
270 from southernmost mooring site off Kanyakumari.

271 **3.1 Southern EAS**

272 At Kanyakumari, with the advent of summer monsoon, the depth of 23°C isotherm (henceforth
273 D23) shallows along-with oxycline (marked by 2.1 ml L^{-1}) and a rise in biomass is observed ([Fig. 4](#)
274 g1). The z175 is shallower during June to September and the zooplankton biomass is comparatively
275 higher than rest of the year. The D175 deepens starting from October and the relatively high
276 biomass in water column is maintained till late December. However, this increase in D175 isn't
277 reflected as an increase in ZSS because of low biomass in the entire water column. A gradual
278 increase is seen in the chlorophyll biomass starting from April and the peak is attained in June
279 ([Fig. 4 g2](#)). The ZSS is increased in June, however the growth is minimal. There is almost no
280 seasonal variation in ZSS off Kanyakumari (seasonal ZSS range, 2.67 gm m^{-2}) as compared to the
281 ZSS variation at the nearest northern mooring site off Kollam (seasonal ZSS range, 4.86 gm m^{-2}),

²⁸² where a strong seasonal cycle is observed and the D215 is deeper for any given month.

²⁸³ Off Kollam, a higher biomass is present in the larger portion of water column and the D215 is
²⁸⁴ at ~ 110 m during Mar-May ([Fig. 4 f1](#)). Similar to z175 off Kanyakumari, the decrease in biomass
²⁸⁵ with depth is subtle below z215. The D215 begins to shallow with progressing summer monsoon.
²⁸⁶ During this period, a sharp decrease is seen in the D23 (~ 60 m in June to September) while
²⁸⁷ the oxycline (1.7 ml L^{-1}) overshoots the thermocline ([Fig. 4. f1](#)). A steep rise in chlorophyll
²⁸⁸ biomass is seen off Kollam and its peak is attained in August ([Fig. 4 f2](#)). The ZSS declines in the
²⁸⁹ same period and reaches a minimum when the chlorophyll biomass is at its peak. The chlorophyll
²⁹⁰ biomass decreases rapidly in the following months, while the ZSS increases and a maximum is seen
²⁹¹ during October. This feature was earlier reported by [[Aparna et al., 2022](#)] showing disproportionate
²⁹² interaction between zooplankton and phytoplankton. It begs the question of existing understanding
²⁹³ of predator - prey relationship in a local-scale ecological system. A similar feature is seen further
²⁹⁴ north, off Udupi which sits at the transition zone of SEAS & CEAS, albeit with a relatively weaker
²⁹⁵ zooplankton biomass. The peak of chlorophyll and minimum of ZSS occurs in September ([Fig. 4 e2](#))
²⁹⁶ which is one month later than off Kollam. The 2.1 ml L^{-1} oxygen contour overshoots thermocline,
²⁹⁷ however it reaches to a much shallow depth of ~ 20 m during July to October. The D200 closely
²⁹⁸ follows D23; with the gradual shallowing from March onward reaching ~ 60 m in September and a
²⁹⁹ steep decline afterwards till November ([Fig. 4 e1](#)). Decrease in biomass with depth is moderate in
³⁰⁰ comparison to Kollam.

³⁰¹ 3.2 Central EAS

³⁰² Off Goa, the D215 seasonal trend is similar to Udupi and is entirely restricted by D23 & oxycline
³⁰³ that closely follows it. During March-May, the D215 is at ~ 100 m which shallows with onset of

³⁰⁴ summer monsoon ([Fig. 4 d1](#)); the chlorophyll biomass increases during this period and the maximum
³⁰⁵ occurs in August after which the chlorophyll biomass and ZSS ([Fig. 5](#)) both decrease in September.
³⁰⁶ Although we witness an increase in chlorophyll biomass in October, the D215 is restricted to the
³⁰⁷ ~ 50 m in this period and the ZSS is at its minimum similar to what is observed off Udupi and
³⁰⁸ Kollam. The ZSS rapidly increases and reaches its maximum in January, sustained till March and
³⁰⁹ then gradually declines. Unlike the previous locations, the biomass off Goa decreases rapidly below
³¹⁰ the z215 as reported earlier [[Aparna et al., 2022](#)], reaching as low as 60 mg m^{-3} during June to
³¹¹ September at 130 m ([Fig. 4 d1](#)).

³¹² The ZSS off Jaigarh is identical but stronger to that off Goa, owing to an higher biomass above
³¹³ z200 and the comparatively deeper D200 ([Fig. 4 c1](#)). The D200 follows D23 & oxycline for most
³¹⁴ of the year and it only exceeds during October-December. From the ZSS maximum in February
³¹⁵ ([Fig. 4 c2](#)), it steadily decreases and attains a minimum in September (coincides with lower D200),
³¹⁶ a rapid rise is seen in the following months. What's intriguing is a presence of strong seasonal cycle
³¹⁷ in ZSS off Jaigarh (10.38 gm m^{-2} , highest among all locations) although the seasonal variation in
³¹⁸ chlorophyll biomass ([Fig. 4 c2](#)) is visibly non-existent (0.15 mg m^{-3} , lowest among all locations).
³¹⁹ This is an exact opposite scenario of Kanyakumari site, where an insignificant seasonal variation in
³²⁰ ZSS (2.67 gm m^{-2}) is seen even though the chlorophyll biomass varies strongly (1.62 mg m^{-3}).

³²¹ Starting from Kollam ([Fig. 4 f1](#)) and moving northward to Jaigarh ([Fig. 4 c1](#)), we see that the
³²² core of high zooplankton biomass gradually shifts from summer monsoon (off Kollam) to winter
³²³ monsoon (off Jaigarh), with the transition of upper ocean zooplankton biomass happening along
³²⁴ Udupi and Goa.

325 **3.3 Northern EAS**

326 Further north of Jaigarh, off Mumbai the D215 follows a similar pattern i.e, a deeper D215 in
327 December to early April, resulting in a higher ZSS in the same period ([Fig. 4 b2](#)). The D23 off
328 Mumbai follows D215 and the oxycline follows an erratic pattern, reaching depths > 140 during
329 January to March ([Fig. 4 b1](#)); when a higher biomass is observed above z215. The chlorophyll
330 biomass shows seasonal variation albeit lower than the SEAS counterpart. Its peak occurs in
331 August, then decreases rapidly and increases from October onward maintaining the biomass at 0.5
332 $mg\ m^{-3}$ till March. In zooplankton biomass climatology, during September-October a thin layer
333 of low biomass regime is seen at depths ~30 - 40 m, combined with shallow D215 resulting in a
334 ZSS minimum. The ZSS increases rapidly from its minima in October in the following month as
335 the D215 deepens and the maximum occurs in February. The chlorophyll biomass decreases from
336 March and a gradual decrease in ZSS is seen till July, after which the ZSS basically flattens even
337 though the chlorophyll increases.

338 At the northernmost site of EAS i.e, off Okha, a noticeable feature is a much higher oxygen in
339 upper ocean. The biomass above z200 is much weaker ([Fig. 4 a1](#)) compared to Mumbai as seen in
340 the zooplankton biomass climatology which leads to a relatively lower ZSS ([Fig. 4 a2](#)). The D200
341 shallows from February (coinciding with ZSS maximum) to its minimum in August, remains visibly
342 flat till September and then increases steadily till December and rapidly afterwards. There's two
343 chlorophyll peak off Okha; one in February [[Keerthi et al., 2017](#)] and the other during August in
344 summer monsoon [[Lévy et al., 2007](#)]. The ZSS remains flat in summer monsoon period i.e, June
345 to September, although the chlorophyll biomass increases in this time. Afterwards, ZSS gradually
346 increases and attains its maximum in February same as the chlorophyll biomass. The ZSS sustains
347 this maximum till March, declines rapidly in April and then gradually till July.

348 **3.4 Comparison to previous result**

349 A comparison with the zooplankton biomass and standing stock climatology of previous work
350 [Aparna et al., 2022] is made in this section for the locations of Mumbai, Goa and Kollam. In the
351 previous study data from 2012 to 2020 is used, while the present study includes data from 2017 to
352 2023.

353 It is observed that D215 is shallower at all locations and as a result a lower ZSS is seen in the
354 climatology of the present study ([Fig. 5](#)). The difference in D215 is prominent off Goa; while in the
355 previous climatology ([Fig. 5 b1](#)) the D215 is deeper and lies along D23, in the present climatological
356 data ([Fig. 5 b2](#)) the D215 is shallower and lies ~ 20 - 40 m above the D23 during January to April.

357 A relatively lower biomass is present above z215 year round which reflects in overall lower ZSS. This
358 goes same for the biomass off Mumbai ([Fig. 5 a1 & a2](#)) i.e, a comparatively shallow D215 and lower
359 ZSS in comparison with [Aparna et al., 2022]. Instead of a ZSS maxima in February, in the present
360 data, the maxima is sustained in march, which could be due to the lower value of ZSS in February.

361 The second maxima occurs in August ([Fig. 5 d1](#)) which is less pronounced in present study ([Fig. 5](#)
362 d2). Similar to Goa, there is dramatic decrease in the minima that occurs in October and ZSS
363 increases rapidly post October till February. Off Kollam, a higher biomass is observed from May to
364 June in previous study, while in the present study, along with May to June, a higher biomass is seen
365 from September to November([Fig. 4 c2](#)) which is reflected as a minima of ZSS occurring in August
366 ([Fig. 4 d2](#)). The higher ZSS on either side to this minima is less pronounced in previous data. This
367 difference in ZSS is clearly seen in the correlation, which is 0.60 off Kollam, while it is 0.94 and 0.98
368 off Mumbai and Goa, respectively. Note that the correlation only shows how similar the ZSS trend

369 is and doesn't tell us about the deviation in magnitude in present study. Chlorophyll biomass shows
370 stronger peak for all locations in August in present study, when the zooplankton-phytoplankton

³⁷¹ relationship discrepancy is observed off Kollam similar to results reported in previous climatology.

³⁷² 4 The seasonal cycle

³⁷³ In the following section we will delineate the seasonal variation of zooplankton biomass and standing
³⁷⁴ stock.

³⁷⁵ 4.1 Seasonal cycle of biomass

³⁷⁶ A preliminary analysis of the biomass time series in daily and monthly averaged scale shows that
³⁷⁷ the biomass decreases with increasing depth ([Fig. 3](#)) at all the seven locations. We've defined depth
³⁷⁸ of

³⁷⁹ The rate of biomass decrease with depth, roughly defined as the difference between the mean
³⁸⁰ biomass at 40 m and 105 m depth, is highest off Jaigarh and Mumbai as it has higher biomass
³⁸¹ in upper ocean ([Fig. 3 c2,b2](#)). This is followed by CEAS locations Goa and Udupi. While the
³⁸² rate of biomass decrease is lower off Kollam for 2017 to 2020. The rate of decrease is lowest off
³⁸³ Kanyakumari. Following is the order of their decrease rate of biomass: Jaigarh (96 mg m^{-3}),
³⁸⁴ Mumbai (91 mg m^{-3}), Okha (79 mg m^{-3}), Udupi (78 mg m^{-3}), Kollam(73 mg m^{-3}), Goa (72
³⁸⁵ mg m^{-3}) and Kanyakumari (39 mg m^{-3}). The mean and standard deviation is shown in [Table 3](#).
³⁸⁶ The weaker decline in zooplankton biomass with respect to the depth at Okha ([Fig. 3 a1,a2](#)) at
³⁸⁷ NEAS is agreeing with earlier reported data [Madhupratap et al. \[2001\]](#), [Smith and Madhupratap](#)
³⁸⁸ [\[2005\]](#), [Wishner et al. \[1998\]](#) where oxygen deficit at is thought to be the cause. The sites at SEAS,
³⁸⁹ especially off Kanyakumari and 2017 to 2020 off Kollam also have weaker decline [[Madhupratap](#)
³⁹⁰ [et al., 2001](#), [Aparna et al., 2022](#)]. However, after 2020 the rate of decline in biomass with depth off
³⁹¹ Kollam is similar to that off Mumbai in stark contrast to its previous years. This is due to a strong

³⁹² bloom in these years also seen at other locations. This high growth led to increase in biomass in
³⁹³ the entire water column([Fig. 3 f1,f2](#)).

³⁹⁴ Analysis of the z215 & z200 shows strong seasonality at the CEAS moorings off Goa and Jaigarh
³⁹⁵ respectively, with low variation in biomass in its upper ocean, with shallow (deeper) D215 & D200
³⁹⁶ in summer (winter) monsoon. This is followed by the moorings off Mumbai and Udupi which are
³⁹⁷ transition zones of NEAS and SEAS, respectively. The

398 **References**

- 399 Anna-Karin Almén and Tobias Tamlander. Temperature-related timing of the spring bloom and match between
400 phytoplankton and zooplankton. *Marine Biology Research*, 16(8-9):674–682, 2020.
- 401 P Amol, D Shankar, V Fernando, A Mukherjee, SG Aparna, R Fernandes, GS Michael, ST Khalap, NP Satelkar,
402 Y Agarvadekar, et al. Observed intraseasonal and seasonal variability of the west india coastal current on the
403 continental slope. *Journal of Earth System Science*, 123(5):1045–1074, 2014.
- 404 P Amol, Suchandan Bemal, D Shankar, V Jain, V Thushara, V Vijith, and PN Vinayachandran. Modulation of
405 chlorophyll concentration by downwelling rossby waves during the winter monsoon in the southeastern arabian
406 sea. *Progress in Oceanography*, 186:102365, 2020.
- 407 SG Aparna, DV Desai, D Shankar, AC Anil, Shrikant Dora, and R Khedekar. Seasonal cycle of zooplankton standing
408 stock inferred from adcp backscatter measurements in the eastern arabian sea. *Progress in Oceanography*, 203:
409 102766, 2022.
- 410 Carin J Ashjian, Sharon L Smith, Charles N Flagg, and Nasseer Idrisi. Distribution, annual cycle, and vertical
411 migration of acoustically derived biomass in the arabian sea during 1994–1995. *Deep Sea Research Part II:*
412 *Topical Studies in Oceanography*, 49(12):2377–2402, 2002.
- 413 K Banse and DC English. Geographical differences in seasonality of czcs-derived phytoplankton pigment in the
414 arabian sea for 1978–1986. *Deep Sea Research Part II: Topical Studies in Oceanography*, 47(7-8):1623–1677, 2000.
- 415 Karl Banse. Hydrography of the arabian sea shelf of india and pakistan and effects on demersal fishes. In *Deep sea*
416 *research and oceanographic Abstracts*, volume 15, pages 45–79. Elsevier, 1968.
- 417 Karl Banse. Zooplankton: pivotal role in the control of ocean production: I. biomass and production. *ICES Journal*
418 *of marine Science*, 52(3-4):265–277, 1995.
- 419 WE Barraclough, RJ LeBrasseur, and OD Kennedy. Shallow scattering layer in the subarctic pacific ocean: detection
420 by high-frequency echo sounder. *Science*, 166(3905):611–613, 1969.
- 421 H. P. Batchelder, J. R. VanKeuren, R. D. Vaillancourt, and E. Swift. Spatial and temporal distributions of acoustically
422 estimated zooplankton biomass near the marine light-mixed layers station (59°30'n, 21°00'w) in the north atlantic
423 in may 1991. *Journal of Geophysical Research: Oceans*, 100:6549–6563, 1995. doi: 10.1029/94jc00981.
- 424 John C Brock and Charles R McClain. Interannual variability in phytoplankton blooms observed in the northwestern
425 arabian sea during the southwest monsoon. *Journal of Geophysical Research: Oceans*, 97(C1):733–750, 1992.
- 426 John C Brock, Charles R McClain, Mark E Luther, and William W Hay. The phytoplankton bloom in the north-
427 western arabian sea during the southwest monsoon of 1979. *Journal of Geophysical Research: Oceans*, 96(C11):
428 20623–20642, 1991.

- 429 Abhisek Chatterjee, D Shankar, SSC Shenoi, GV Reddy, GS Michael, M Ravichandran, VV Gopalkrishna,
430 EP Rama Rao, TVS Udaya Bhaskar, and VN Sanjeevan. A new atlas of temperature and salinity for the north
431 indian ocean. *Journal of Earth System Science*, 121:559–593, 2012.
- 432 Anya Chaudhuri, D Shankar, SG Aparna, P Amol, V Fernando, A Kankonkar, GS Michael, NP Satelkar, ST Khalap,
433 AP Tari, et al. Observed variability of the west india coastal current on the continental slope from 2009–2018.
434 *Journal of Earth System Science*, 129(1):57, 2020.
- 435 Anya Chaudhuri, P Amol, D Shankar, S Mukhopadhyay, SG Aparna, V Fernando, and A Kankonkar. Observed
436 variability of the west india coastal current on the continental shelf from 2010–2017. *Journal of Earth System
437 Science*, 130:1–21, 2021.
- 438 Boris Cisewski, Volker H Strass, Monika Rhein, and Sören Krägesky. Seasonal variation of diel vertical migration
439 of zooplankton from adcp backscatter time series data in the lazarev sea, antarctica. *Deep Sea Research Part I:
440 Oceanographic Research Papers*, 57(1):78–94, 2010.
- 441 Kent L Deines. Backscatter estimation using broadband acoustic doppler current profilers. In *Proceedings of the
442 IEEE Sixth Working Conference on Current Measurement (Cat. No. 99CH36331)*, pages 249–253. IEEE, 1999.
- 443 A Edvardsen, D Slagstad, KS Tande, and P Jaccard. Assessing zooplankton advection in the barents sea using
444 underway measurements and modelling. *Fisheries Oceanography*, 12(2):61–74, 2003.
- 445 S Fielding, G Griffiths, and HSJ Roe. The biological validation of adcp acoustic backscatter through direct comparison
446 with net samples and model predictions based on acoustic-scattering models. *ICES Journal of Marine Science*,
447 61(2):184–200, 2004.
- 448 Charles N Flagg and Sharon L Smith. On the use of the acoustic doppler current profiler to measure zooplankton
449 abundance. *Deep Sea Research Part A. Oceanographic Research Papers*, 36(3):455–474, 1989.
- 450 H. E. García, R. A. Locarnini, T. P. Boyer, J. I. Antonov, A. V. Mishonov, O. K. Baranova, M. M. Zweng, J. R.
451 Reagan, and D. R. Johnson. Dissolved oxygen, apparent oxygen utilization, and oxygen saturation. *NOAA Atlas
452 NESDIS 75*, 3, 2014.
- 453 Charles H Greene, Peter H Wiebe, Chris Pelkie, Mark C Benfield, and Jacqueline M Popp. Three-dimensional
454 acoustic visualization of zooplankton patchiness. *Deep Sea Research Part II: Topical Studies in Oceanography*, 45
455 (7):1201–1217, 1998.
- 456 Charles F Greenlaw. Acoustical estimation of zooplankton populations 1. *Limnology and Oceanography*, 24(2):
457 226–242, 1979.
- 458 Davide Guerra, Katrin Schroeder, Mireno Borghini, Elisa Camatti, Marco Pansera, Anna Schroeder, Stefania
459 Sparnocchia, and Jacopo Chiggiato. Zooplankton diel vertical migration in the corsica channel (north-western
460 mediterranean sea) detected by a moored acoustic doppler current profiler. *Ocean Science*, 15(3):631–649, 2019.

- 461 Graeme C Hays. A review of the adaptive significance and ecosystem consequences of zooplankton diel vertical
462 migrations. In *Migrations and Dispersal of Marine Organisms: Proceedings of the 37 th European Marine Biology*
463 *Symposium held in Reykjavik, Iceland, 5–9 August 2002*, pages 163–170. Springer, 2003.
- 464 PJ Herring, MJR Fasham, AR Weeks, JCP Hemmings, HSJ Roe, PR Pugh, S Holley, NA Crisp, and MV Angel.
465 Across-slope relations between the biological populations, the euphotic zone and the oxygen minimum layer off
466 the coast of oman during the southwest monsoon (august, 1994). *Progress in Oceanography*, 41(1):69–109, 1998.
- 467 Karen J Heywood, S Scrope-Howe, and ED Barton. Estimation of zooplankton abundance from shipborne adcp
468 backscatter. *Deep Sea Research Part A. Oceanographic Research Papers*, 38(6):677–691, 1991.
- 469 Laura Hobbs, Neil S Banas, Jonathan H Cohen, Finlo R Cottier, Jørgen Berge, and Øystein Varpe. A marine
470 zooplankton community vertically structured by light across diel to interannual timescales. *Biology Letters*, 17(2):
471 20200810, 2021.
- 472 Raleigh R Hood, Lynnath E Beckley, and Jerry D Wiggert. Biogeochemical and ecological impacts of boundary
473 currents in the indian ocean. *Progress in Oceanography*, 156:290–325, 2017.
- 474 Ryuichiro Inoue, Minoru Kitamura, and Tetsuichi Fujiki. Diel vertical migration of zooplankton at the s 1 biogeo-
475 chemical mooring revealed from acoustic backscattering strength. *Journal of Geophysical Research: Oceans*, 121
476 (2):1031–1050, 2016.
- 477 Songnian Jiang, Tommy D Dickey, Deborah K Steinberg, and Laurence P Madin. Temporal variability of zooplankton
478 biomass from adcp backscatter time series data at the bermuda testbed mooring site. *Deep Sea Research Part I:*
479 *Oceanographic Research Papers*, 54(4):608–636, 2007.
- 480 R Jyothibabu, NV Madhu, H Habeebrehman, KV Jayalakshmy, KKC Nair, and CT Achuthankutty. Re-evaluation
481 of ‘paradox of mesozooplankton’ in the eastern arabian sea based on ship and satellite observations. *Journal of*
482 *Marine Systems*, 81(3):235–251, 2010.
- 483 Myounghee Kang, Sunyoung Oh, Wooseok Oh, Dong-Jin Kang, SungHyun Nam, and Kyounghoon Lee. Acoustic
484 characterization of fish and macroplankton communities in the seychelles-chagos thermocline ridge of the southwest
485 indian ocean. *Deep Sea Research Part II: Topical Studies in Oceanography*, 213:105356, 2024.
- 486 Madhavan Girijakumari Keerthi, Matthieu Lengaigne, Marina Levy, Jerome Vialard, Vallivattathillam Parvathi,
487 Clément de Boyer Montégut, Christian Ethé, Olivier Aumont, Iyyappan Suresh, Valiya Parambil Akhil, et al.
488 Physical control of interannual variations of the winter chlorophyll bloom in the northern arabian sea. *Biogeosciences*, 14(15):3615–3632, 2017.
- 490 Corinne Le Qu, Robbie M Andrew, Josep G Canadell, Stephen Sitch, Jan Ivar Korsbakken, Glen P Peters, Andrew C
491 Manning, Thomas A Boden, Pieter P Tans, Richard A Houghton, et al. Global carbon budget 2016. *Earth System*
492 *Science Data*, 8(2):605–649, 2016.

- 493 Marina Lévy, D Shankar, J-M André, SSC Shenoi, Fabien Durand, and Clément de Boyer Montégut. Basin-wide
494 seasonal evolution of the indian ocean's phytoplankton blooms. *Journal of Geophysical Research: Oceans*, 112
495 (C12), 2007.
- 496 M Li, A Gargett, and K Denman. What determines seasonal and interannual variability of phytoplankton and
497 zooplankton in strongly estuarine systems? *Estuarine, Coastal and Shelf Science*, 50(4):467–488, 2000.
- 498 Yanliang Liu, Jingsong Guo, Yuhuan Xue, Chalermrat Sangmanee, Huiwu Wang, Chang Zhao, Somkiat Khokiat-
499 tiwong, and Weidong Yu. Seasonal variation in diel vertical migration of zooplankton and micronekton in the
500 andaman sea observed by a moored adcp. *Deep Sea Research Part I: Oceanographic Research Papers*, 179:103663,
501 2022.
- 502 M Madhupratap, P Haridas, Neelam Ramaiah, and CT Achuthankutty. Zooplankton of the southwest coast of india:
503 abundance, composition, temporal and spatial variability in 1987. 1992.
- 504 M Madhupratap, TC Gopalakrishnan, P Haridas, KKC Nair, PN Aravindakshan, G Padmavati, and Shiney Paul.
505 Lack of seasonal and geographic variation in mesozooplankton biomass in the arabian sea and its structure in the
506 mixed layer. *Current science. Bangalore*, 71(11):863–868, 1996a.
- 507 M Madhupratap, S Prasanna Kumar, PMA Bhattachari, M Dileep Kumar, S Raghukumar, KKC Nair, and N Rama-
508 iah. Mechanism of the biological response to winter cooling in the northeastern arabian sea. *Nature*, 384(6609):
509 549–552, 1996b.
- 510 M Madhupratap, TC Gopalakrishnan, P Haridas, and KKC Nair. Mesozooplankton biomass, composition and
511 distribution in the arabian sea during the fall intermonsoon: implications of oxygen gradients. *Deep Sea Research
512 Part II: Topical Studies in Oceanography*, 48(6-7):1345–1368, 2001.
- 513 PA Maheswaran, G Rajesh, C Revichandran, and KKC Nair. Upwelling and associated hydrography along the west
514 coast of india during southwest monsoon, 1999. 2000.
- 515 JP McCreary, Raghu Murtugudde, Jerome Vialard, PN Vinayachandran, Jerry D Wiggert, Raleigh R Hood,
516 D Shankar, and S Shetye. Biophysical processes in the indian ocean. *Indian Ocean biogeochemical processes
517 and ecological variability*, 185:9–32, 2009.
- 518 Julian P McCreary Jr, Pijush K Kundu, and Robert L Molinari. A numerical investigation of dynamics, thermody-
519 namics and mixed-layer processes in the indian ocean. *Progress in Oceanography*, 31(3):181–244, 1993.
- 520 Donald C McNaught. Acoustical determination of zooplankton distribution. In *Proc. 11th Conf. Great lakes Res.*,
521 pages 76–84, 1968.
- 522 A Mukherjee, D Shankar, V Fernando, P Amol, SG Aparna, R Fernandes, GS Michael, ST Khalap, NP Satelkar,
523 Y Agarvadekar, et al. Observed seasonal and intraseasonal variability of the east india coastal current on the
524 continental slope. *Journal of Earth System Science*, 123(6):1197–1232, 2014.

- 525 S Mukhopadhyay, D Shankar, SG Aparna, A Mukherjee, V Fernando, A Kankonkar, S Khalap, NP Satelkar,
526 MG Gaonkar, AP Tari, et al. Observed variability of the east india coastal current on the continental slope
527 during 2009–2018. *Journal of Earth System Science*, 129:1–22, 2020.
- 528 Jerry Mullison. Backscatter estimation using broadband acoustic doppler current profilers-updated. In *Proceedings*
529 *of the ASCE Hydraulic Measurements & Experimental Methods Conference, Durham, NH, USA*, pages 9–12,
530 2017.
- 531 KKC Nair, M Madhupratap, TC Gopalakrishnan, P Haridas, and Mangesh Gauns. The arabian sea: physical
532 environment, zooplankton and myctophid abundance. 1999.
- 533 PV Nair. Primary productivity in the indian seas. *CMFRI Bulletin*, 22:1–63, 1970.
- 534 Lingyun Nie, Jianchao Li, Hao Wu, Wenchao Zhang, Yongjun Tian, Yang Liu, Peng Sun, Zhenjiang Ye, Shuyang
535 Ma, and Qinfeng Gao. The influence of ocean processes on fine-scale changes in the yellow sea cold water mass
536 boundary area structure based on acoustic observations. *Remote Sensing*, 15(17):4272, 2023.
- 537 MD Ohman and H-J Hirche. Density-dependent mortality in an oceanic copepod population. *Nature*, 412(6847):
538 638–641, 2001.
- 539 G Padmavati, P Haridas, KKC Nair, TC Gopalakrishnan, P Shiney, and M Madhupratap. Vertical distribution of
540 mesozooplankton in the central and eastern arabian sea during the winter monsoon. *Journal of Plankton Research*,
541 20(2):343–354, 1998.
- 542 MR Patil, CP Ramamirtham, P Udaya Varma, and CP Nair. Hydrography of the west coast of india during the
543 pre-monsoon period of the year 1962. *Journal of marine biological association of India*, 6(1):151–164, 1964.
- 544 Richard Edward Pieper. *A study of the relationship between zooplankton and high-frequency scattering of underwater*
545 *sound*. PhD thesis, University of British Columbia, 1971.
- 546 SA Piontkovski, R Williams, and TA Melnik. Spatial heterogeneity, biomass and size structure of plankton of the
547 indian ocean: some general trends. *Marine ecology progress series*, pages 219–227, 1995.
- 548 Emmanuel Potiris, Constantin Frangoulis, Alkiviadis Kalampokis, Manolis Ntoumas, Manos Pettas, George Peti-
549 hakis, and Vassilis Zervakis. Acoustic doppler current profiler observations of migration patterns of zooplankton
550 in the cretan sea. *Ocean Science*, 14(4):783–800, 2018.
- 551 SZ Qasim. Biological productivity of the indian ocean. 1977.
- 552 CP Ramamirtham and AVS Murty. Hydrography of the west coast of india during the pre-monsoon period of the
553 year 1962—part 2: in and offshore waters of the konkan and malabar coasts. *Journal of the Marine Biological*
554 *Association of India*, 7(1):150–168, 1965.
- 555 S Ramamurthy. Studies on the plankton of the north kanara coast in relation to the pelagic fishery. *Journal of*
556 *Marine Biological Association of India*, 7(1):127–149, 1965.

- 557 Mehbuba Rehim and Mudassar Imran. Dynamical analysis of a delay model of phytoplankton–zooplankton interac-
558 tion. *Applied Mathematical Modelling*, 36(2):638–647, 2012.
- 559 T. P. Rippeth and J. H. Simpson. Diurnal signals in vertical motions on the hebridean shelf. *Limnology and*
560 *Oceanography*, 43:1690–1696, 1998. doi: 10.4319/lo.1998.43.7.1690.
- 561 John H Ryther, John R Hall, Allan K Pease, Andrew Bakun, and Mark M Jones. Primary organic production in
562 relation to the chemistry and hydrography of the western indian ocean 1. *Limnology and Oceanography*, 11(3):
563 371–380, 1966.
- 564 D Sameoto and S Paulowich. The use of 120 khz sonar in zooplankton studies. In *OCEANS'77 Conference Record*,
565 pages 523–528. IEEE, 1977.
- 566 D Shankar and SR Shetye. On the dynamics of the lakshadweep high and low in the southeastern arabian sea.
567 *Journal of Geophysical Research: Oceans*, 102(C6):12551–12562, 1997.
- 568 D Shankar, R Remya, PN Vinayachandran, Abhisek Chatterjee, and Ambica Behera. Inhibition of mixed-layer
569 deepening during winter in the northeastern arabian sea by the west india coastal current. *Climate Dynamics*,
570 47:1049–1072, 2016.
- 571 D Shankar, R Remya, AC Anil, and V Vijith. Role of physical processes in determining the nature of fisheries in the
572 eastern arabian sea. *Progress in Oceanography*, 172:124–158, 2019.
- 573 SR Shetye and AD Gouveia. Coastal circulation in the north indian ocean: Coastal segment (14, sw). John Wiley
574 and Sons, New York, USA, 1998.
- 575 SR Shetye, AD Gouveia, SSC Shenoi, D Sundar, GS Michael, AM Almeida, and K Santanam. Hydrography and
576 circulation off the west coast of india during the southwest monsoon 1987. 1990.
- 577 SR Shetye, AD Gouveia, SSC Shenoi, GS Michael, D Sundar, AM Almeida, and K Santanam. The coastal current
578 off western india during the northeast monsoon. *Deep Sea Research Part A. Oceanographic Research Papers*, 38
579 (12):1517–1529, 1991.
- 580 SR Shetye, AD Gouveia, and SSC Shenoi. Does winter cooling lead to the subsurface salinity minimum off saurashtra,
581 india? *Oceanography of the Indian Ocean*, pages 617–625, 1992.
- 582 Greg M Silsbe, Michael J Behrenfeld, Kimberly H Halsey, Allen J Milligan, and Toby K Westberry. The cafe model:
583 A net production model for global ocean phytoplankton. *Global Biogeochemical Cycles*, 30(12):1756–1777, 2016.
- 584 Houssem Smeti, Marc Pagano, Christophe Menkes, Anne Lebourges-Dhaussy, Brian PV Hunt, Valerie Allain, Martine
585 Rodier, Florian De Boissieu, Elodie Kestenare, and Cherif Sammari. Spatial and temporal variability of zooplank-
586 ton off n ew c alifornia (s outhwestern p acific) from acoustics and net measurements. *Journal of Geophysical*
587 *Research: Oceans*, 120(4):2676–2700, 2015.

- 588 SL Smith and M Madhupratap. Mesozooplankton of the arabian sea: patterns influenced by seasons, upwelling, and
589 oxygen concentrations. *Progress in Oceanography*, 65(2-4):214–239, 2005.
- 590 Patnaik Sreenivas, KVKRK Patnaik, and KVSR Prasad. Monthly variability of mixed layer over arabian sea using
591 argo data. *Marine Geodesy*, 31(1):17–38, 2008.
- 592 R Subrahmanyam. Studies on the phytoplankton of the west coast of india: Part ii. physical and chemical factors
593 influencing the production of phytoplankton, with remarks on the cycle of nutrients and on the relationship of
594 the phosphate-content to fish landings. In *Proceedings/Indian Academy of Sciences*, volume 50, pages 189–252.
595 Springer, 1959.
- 596 R Subrahmanyam and AH Sarma. Studies on the phytoplankton of the west coast of india. part iii. seasonal variation
597 of the phytoplankters and environmental factors. *Indian Journal of Fisheries*, 7(2):307–336, 1960.
- 598 Laura Ursella, Vanessa Cardin, Mirna Batistić, Rade Garić, and Miroslav Gačić. Evidence of zooplankton vertical
599 migration from continuous southern adriatic buoy current-meter records. *Progress in oceanography*, 167:78–96,
600 2018.
- 601 Laura Ursella, Sara Pensieri, Enric Pallàs-Sanz, Sharon Z Herzka, Roberto Bozzano, Miguel Tenreiro, Vanessa Cardin,
602 Julio Candela, and Julio Sheinbaum. Diel, lunar and seasonal vertical migration in the deep western gulf of mexico
603 evidenced from a long-term data series of acoustic backscatter. *Progress in Oceanography*, 195:102562, 2021.
- 604 V Vijith, PN Vinayachandran, V Thushara, P Amol, D Shankar, and AC Anil. Consequences of inhibition of mixed-
605 layer deepening by the west india coastal current for winter phytoplankton bloom in the northeastern arabian sea.
606 *Journal of Geophysical Research: Oceans*, 121(9):6583–6603, 2016.
- 607 Peter H Wiebe, Charles H Greene, Timothy K Stanton, and Janusz Burczynski. Sound scattering by live zooplankton
608 and micronekton: empirical studies with a dual-beam acoustical system. *The Journal of the Acoustical Society of
609 America*, 88(5):2346–2360, 1990.
- 610 Monika Winder and Daniel E Schindler. Climatic effects on the phenology of lake processes. *Global change biology*,
611 10(11):1844–1856, 2004.
- 612 Karen F Wishner, Marcia M Gowing, and Celia Gelfman. Mesozooplankton biomass in the upper 1000 m in the
613 arabian sea: overall seasonal and geographic patterns, and relationship to oxygen gradients. *Deep Sea Research
614 Part II: Topical Studies in Oceanography*, 45(10-11):2405–2432, 1998.

Table 1: ADCP deployment details at the locations. The temporal resolution is 1 hour, bin size(vertical resolution) 4 m. All ADCPs are operated at 153.3 kHz. The moorings are at a water column depth of 950 - 1200 m on the continental slope and are serviced on yearly basis according to ship availability. The 6th column consists of Reference echo intensity (Er) for each beam, while the 7th column contains the corresponding RSSI conversion factor [Deines, 1999].

Station (Position; °E, °N)	Date			Depth		Er
	Deployment	Recovery	Ocean	ADCP		
Okha (67.47, 22.26)	01/10/2018	01/12/2019	996	118	37 , 37 , 37 , 36	0.42 ,
	01/12/2019	04/12/2020	1166	312	39 , 36 , 38 , 36	0.42 ,
	04/12/2020	08/03/2022	1021	144	41 , 37 , 38 , 37	0.42 ,
	08/03/2022	01/01/2023	1019	142	37 , 38 , 39 , 36	0.42 ,
Mumbai (69.24, 20.01)	09/11/2017	29/09/2018	1025	150	36 , 34 , 39 , 42	0.40 ,
	29/09/2018	29/11/2019	1122	125	35 , 36 , 39 , 42	0.40 ,
	29/11/2019	02/12/2020	1143	164	37 , 34 , 39 , 43	0.40 ,
	02/12/2020	06/03/2022	1125	142	36 , 34 , 39 , 42	0.40 ,
	07/03/2022	02/01/2023	1103	158	37 , 34 , 40 , 43	0.40 ,
Jaigarh (71.12, 17.53)	27/10/2017	27/09/2018	1039	198	32 , 35 , 33 , 32	0.45 ,
	27/09/2018	30/10/2019	1032	164	32 , 35 , 33 , 31	0.45 ,
	03/11/2019	30/11/2020	1142	264	32 , 36 , 33 , 32	0.45 ,
	30/11/2020	05/03/2022	1099	119	33 , 36 , 34 , 32	0.45 ,
Goa (72.74, 15.17)	03/10/2017	25/09/2018	1000	174 this has to be updated to include later samples		35 , 37 , 34 , 35
	25/09/2018	16/10/2019	969	145	38 , 36 , 36 , 34	0.44 ,
	16/10/2019	29/11/2020	966	143	44 , 38 , 36 , 43	0.44 ,
	29/11/2020	03/03/2022	985	157	35 , 40 , 35 , 38	0.44 ,
	03/03/2022	05/01/2023	984	159	35 , 38 , 35 , 34	0.44 ,
Udupi (74.04, 12.5)	05/10/2017	06/10/2018	1028	176	44 , 46 , 29 , 35	0.45 ,
	06/10/2018	18/10/2019	1027	179	32 , 38 , 30 , 36	0.45 ,
	18/10/2019	11/12/2020	1018	168	33 , 37 , 31 , 38	0.45 ,
	11/03/2022	06/01/2023	1036	155	31 , 32 , 32 , 33	0.45 ,
Kollam (75.44, 9.05)	07/10/2017	08/10/2018	1174	200	43 , 55 , 45 , 43	0.49 ,
	08/10/2018	20/10/2019	1160	123	49 , 62 , 46 , 46	0.49 ,
	20/10/2019	13/12/2020	1209	176	52 , 61 , 54 , 55	0.49 ,
	13/12/2020	13/03/2022	1129	91	49 , 51 , 46 , 47	0.49 ,
	13/03/2022	08/01/2023	1149	164	41 , 48 , 43 , 41	0.49 ,
Kanyakumari (77.39, 6.96)	16/11/2016	08/10/2017	1096	252	37 , 36 , 37 , 37	0.42 ,
	08/10/2017	10/10/2018	1055	181	32 , 34 , 38 , 35	0.45 ,
	10/10/2018	22/10/2019	1075	180	36 , 34 , 39 , 36	0.45 ,
	22/10/2019	14/12/2020	1060	167	33 , 35 , 36 , 35	0.45 ,
	14/12/2020	14/03/2022	1184	287	34 , 36 , 36 , 35	0.45 ,

Table 2:

Volumetric samples of zooplankton of various stations. The sampling depth range is standardised for later years for bin range of 0–25m, 25–50m, 50–75m, 75–100m, 100–150m. The abbreviations are in the following manner: Okha (O), Mumbai (M), Jaigarh (J), Goa (G), Udupi (U), Kollam (K), Kanyakumari (KK); The number tags corresponds to particular cruise of a station.

Sample number	Tag	Lat($^{\circ}$ N)	Lon($^{\circ}$ E)	Date	Time (IST)	Sampling depth range (m)
1-3	G1	15.18	72.79	25 Sep 18	452	50–25, 100–50, 150–100
4-6	G2	15.16	72.71	25 Sep 18	2108	50–25, 100–50, 150–100
7-10	G2	15.16	72.71	25 Sep 18	2137	40–20, 60–40, 80–60, 100–80
11-14	J1			26 Sep 18	2000	40–20, 60–40, 80–60, 100–80
15-17	J2			27 Sep 18	2000	50–25, 100–50, 150–100
18-21	J2			27 Sep 18	2100	40–20, 60–40, 80–60, 100–80
22-25	M1	20	69.19	28 Sep 18	2135	40–20, 60–40, 80–60, 100–80
26-27	M1	20	69.19	28 Sep 18	2205	50–25, 100–50
28-29	M2	20.01	69.2	29 Sep 18	2035	50–25, 100–50
30-33	M2	20.01	69.2	29 Sep 18	2057	40–20, 60–40, 80–60, 100–80
34-37	U1			5 Oct 18	2000	40–20, 60–40, 80–60, 100–80
38-40	U1			5 Oct 18	2100	50–25, 100–50, 150–100
41-43	U2			6 Oct 18	2000	50–25, 100–50, 150–100
44-47	U2			6 Oct 18	2100	40–20, 60–40, 80–60, 100–80
48-51	K1	9.06	75.42	8 Oct 18	421	40–20, 60–40, 80–60, 100–80
52-54	K1	9.06	75.42	8 Oct 18	449	50–25, 100–50, 150–100
55-56	K2	9.04	75.4	8 Oct 18	2027	50–25, 100–50
57-60	K2	9.04	75.4	8 Oct 18	2045	40–20, 60–40, 80–60, 100–80
61-64	G2	15.16	72.74	16 Oct 19	829	50–25, 75–50, 100–75, 150–100
65-67	G3	15.16	72.74	16 Oct 19	1812	50–25, 75–50, 100–75
68-70	K2	9.02	75.42	20 Oct 19	840	50–25, 75–50, 100–75
71-74	K3	9.04	75.43	20 Oct 19	1934	50–25, 75–50, 100–75, 150–100
75-78	KK1			22 Oct 19	742	50–25, 75–50, 100–75, 150–100
79-82	KK2			22 Oct 19	1925	50–25, 75–50, 100–75, 150–100
83-86	J1			30 Oct 19	324	50–25, 75–50, 100–75, 150–100
87-89	J2			4 Nov 19	946	75–50, 100–75, 150–100
90-92	M2	19.98	69.22	29 Nov 19	1434	50–25, 75–50, 100–75
93-96	M3	20.01	69.23	30 Nov 19	958	50–25, 75–50, 100–75, 150–100
97-100	O1	22.24	67.49	1 Dec 19	937	50–25, 75–50, 100–75, 150–100
101	O2	22.25	67.46	1 Dec 19	1957	150–100
102-105	G3	15.68	73.22	28 Nov 20	930	50–25, 75–50, 100–75, 150–100
105-108	G4	15.32	73.22	29 Nov 20	1558	50–25, 75–50, 100–75, 150–100
108-110	J2	17.85	71.21	30 Nov 20	1458	75–50, 100–75, 150–100
111-114	J3	17.91	71.21	1 Dec 20	1052	50–25, 75–50, 100–75, 150–100
115-118	M4	20.03	69.38	2 Dec 20	2016	50–25, 75–50, 100–75, 150–100
119-00	O2	22.41	67.8	4 Dec 20	953	150–100
120-123	O3	22.41	67.79	4 Dec 20	2011	50–25, 75–50, 100–75, 150–100
124-127	K3	9.11	75.72	12 Dec 20	2335	50–25, 75–50, 100–75, 150–100
128-131	K4	9.06	75.74	13 Dec 20	1507	50–25, 75–50, 100–75, 150–100
132-134	KK1	7.62	77.63	14 Dec 20	1226	50–25, 75–50
135-138	KK2	7.62	77.63	14 Dec 20	2047	50–25, 75–50, 100–75, 150–100
139-142	G4	15.32	73.21	3 Mar 22	823	50–25, 75–50, 100–75, 150–100
143-146	G5	15.68	73.21	4 Mar 22	1030	50–25, 75–50, 100–75, 150–100
147-150	M5	19.99	69.23	7 Mar 22	957	50–25, 75–50, 100–75, 150–100
151-154	O3	22.24	67.5	8 Mar 22	806	50–25, 75–50, 100–75, 150–100
155-158	U3	12.5	74.04	12 Mar 22	1156	50–25, 75–50, 100–75, 150–100
159-160	K4	9.04	75.42	13 Mar 22	1027	50–25, 75–50, 100–75
161-164	KK3	6.97	77.4	15 Mar 22	1220	50–25, 75–50, 100–75, 150–100

Table 3:
 The mean, standard deviation at 40 and 104 m of biomass at 7 mooring sites and their difference is tabulated. All units are in $mg\ m^{-3}$.

	40 m		104 m		
	Mean	std	Mean	std	difference
Okha	230.42	22.84	151.68	25.58	78.74
Mumbai	272.86	34.95	182.24	30.34	90.62
Jaigarh	278.45	36.52	182.96	48.89	95.49
Goa	235.22	30.34	163.02	36.54	72.2
Udupi	247.81	34.37	169.37	38.8	78.43
Kollam	272.56	54.94	198.89	50.08	73.67
Kanyakumari	207.07	30.42	167.63	20.89	39.44

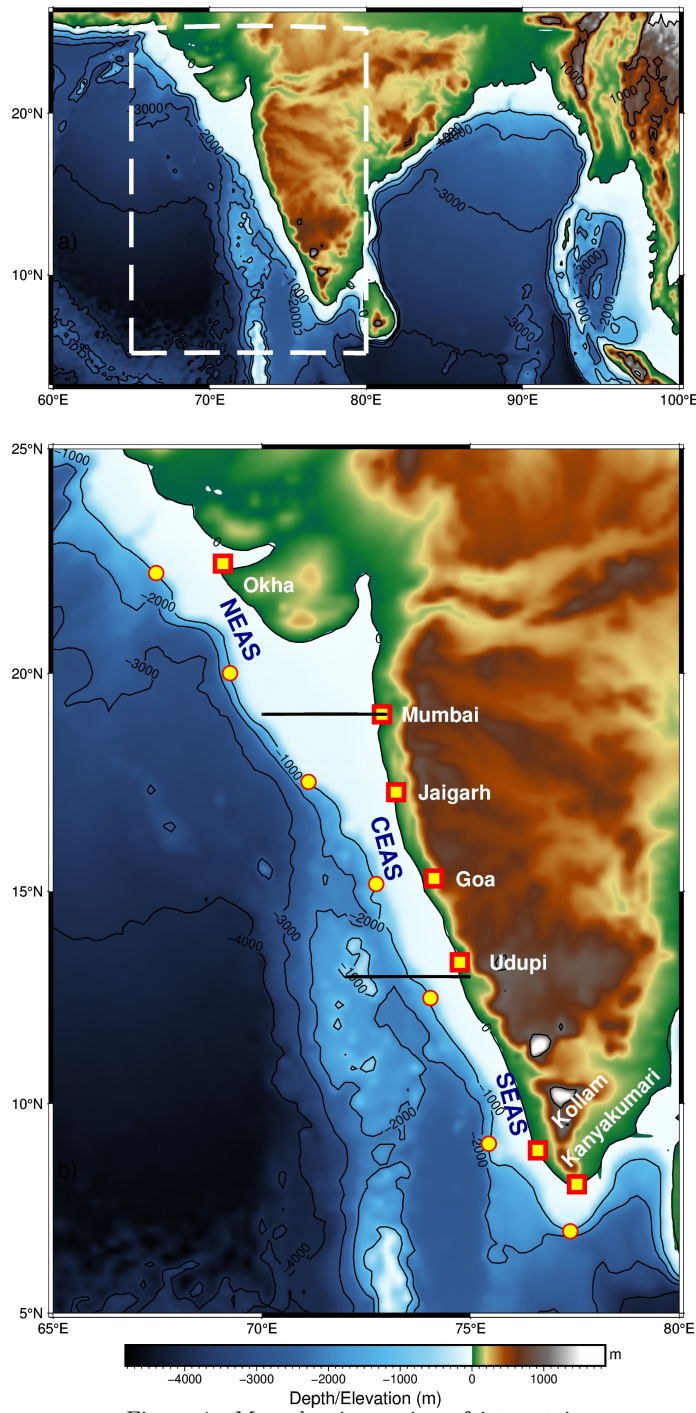


Figure 1: Map showing region of interest in eastern Arabian Sea. The slope moorings are deployed at 1000 m depth as shown in the bathymetry contour.

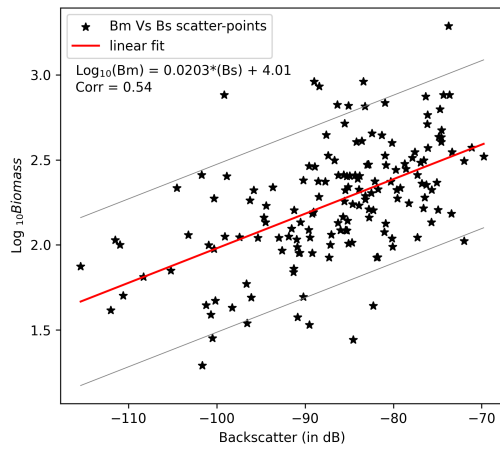


Figure 2: The linear fit line of Biomass (scale of log) and backscattering strength (in dB). The linear fit line is within the error range of previous result of [Aparna et al., 2022] onto which latest zooplankton volumetric sample data is added.

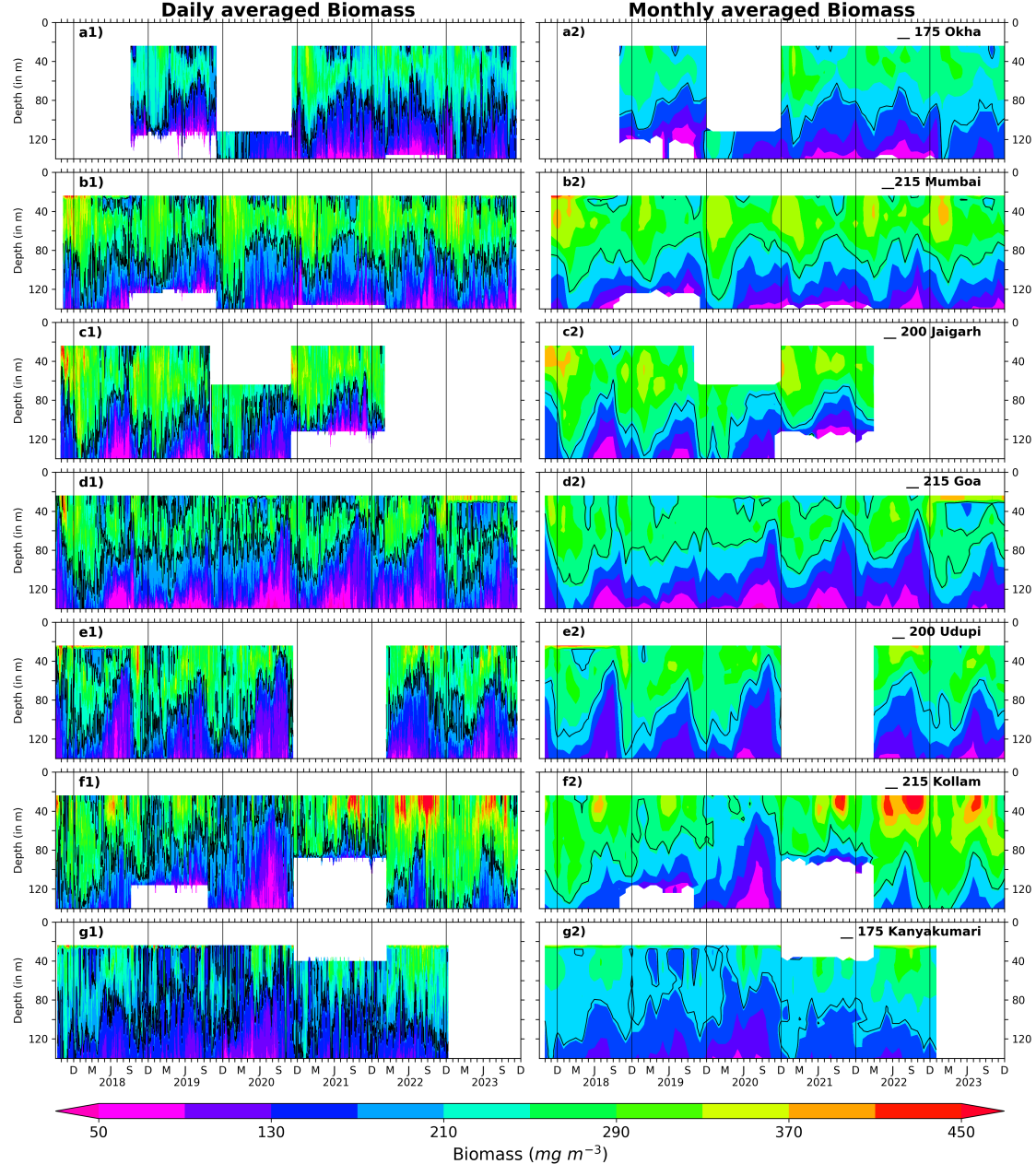


Figure 3: The Daily and monthly averaged biomass for EAS moorings, north (top) to south (bottom). The black contours are marking of 175 mg m^{-3} biomass for Okha and Kanyakumari; 200 mg m^{-3} for Jaigarh and Udupi; 215 mg m^{-3} for Mumbai, Goa and Kollam. The biomass contours are distinct and different based on the physico-chemical parameters and the one that best explains seasonality at respective location.

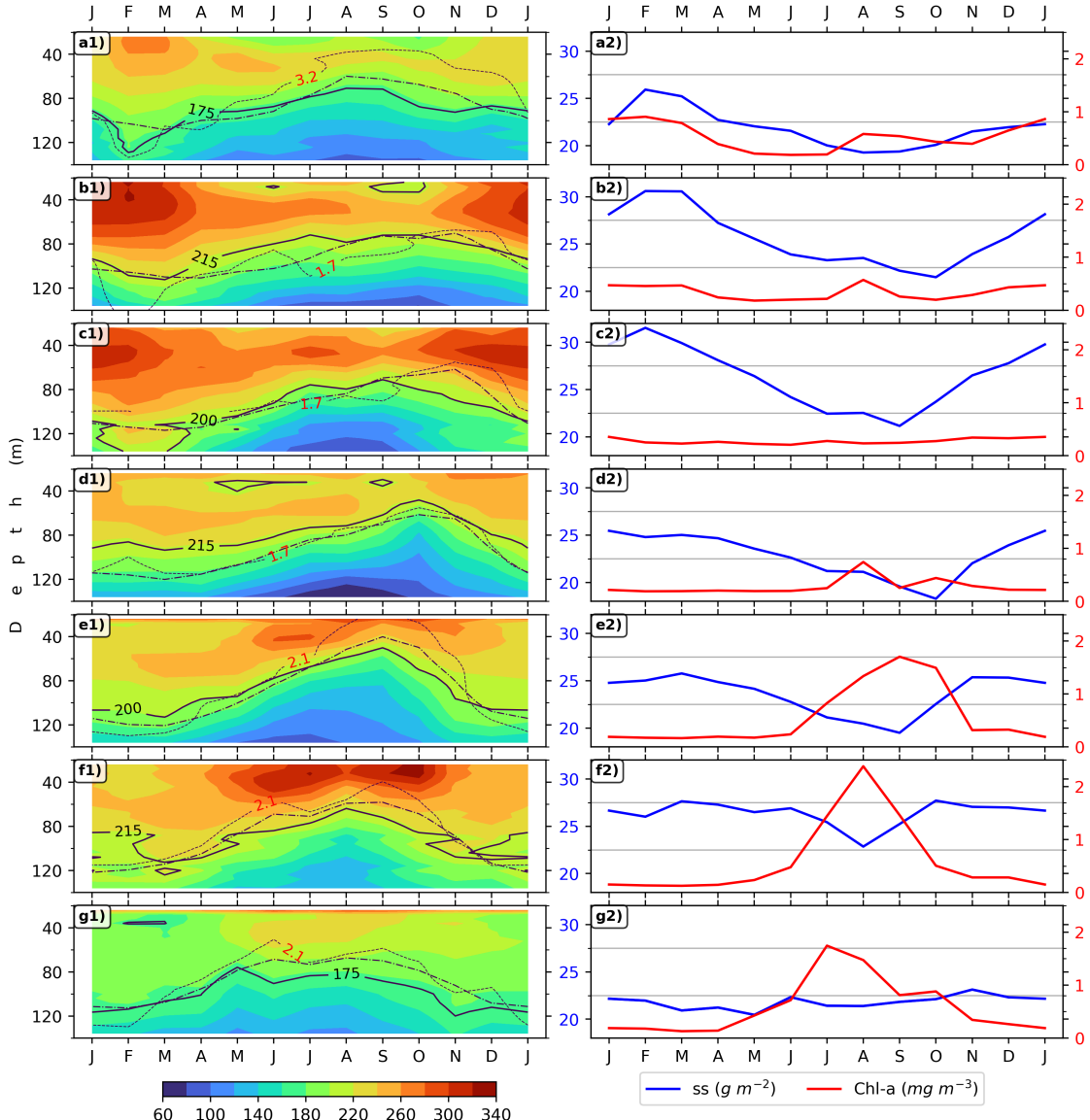


Figure 4: Monthly climatology of zooplankton biomass is shown in left panels for 7 locations, (top to bottom is southward). The D175, D200 & D215 are shown in solid lines; dashed line represents the depth of 23 °C isotherm; oxygen contours are shown in dotted lines and labeled for each mooring. The plot labels are as follows: a1 & a2 for Okha, b1 & b2 for Mumbai, c1 & c2 for Jaigarh, d1 & d2 for Goa, e1 & e2 for Udupi, f1 & f2 for Kollam, g1 & g2 for Kanyakumari. The right set of panel plots is showing ZSS and chlorophyll climatology for respective locations.

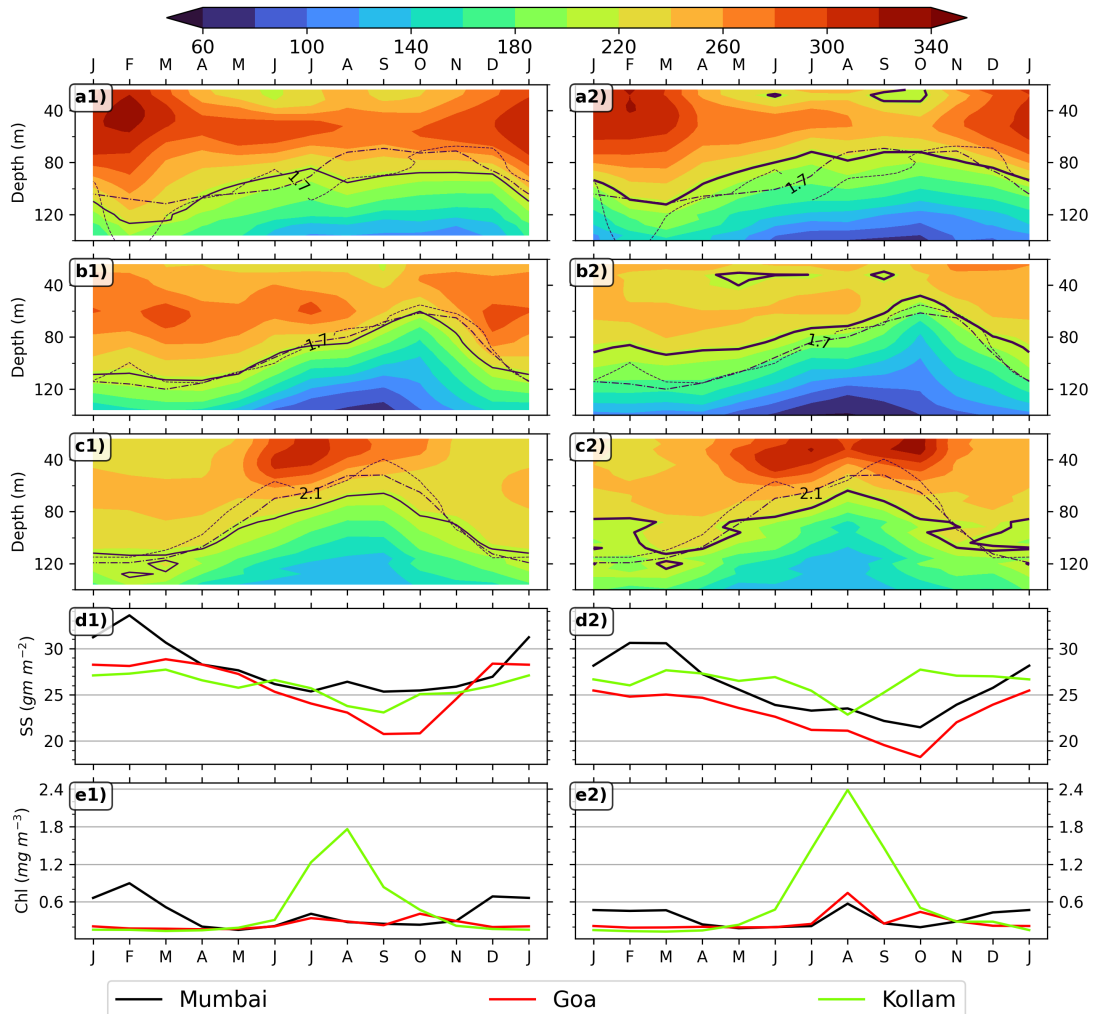


Figure 5: Monthly climatology of zooplankton biomass is shown in left panels for 3 locations which were earlier used in [Aparna et al., 2022]; a1, b1 & c1 is the biomass climatology for Mumbai, Goa and Kollam, d1 is for ZSS climatology, e1 is for chlorophyll biomass climatology; a2, b2, c2, d2 & e2 is same but based on data from 2017 to 2023. The D215 is shown in solid line. The dashed line represents the depth of 23 °C isotherm; oxygen contours are shown in dotted lines and labeled for each mooring.

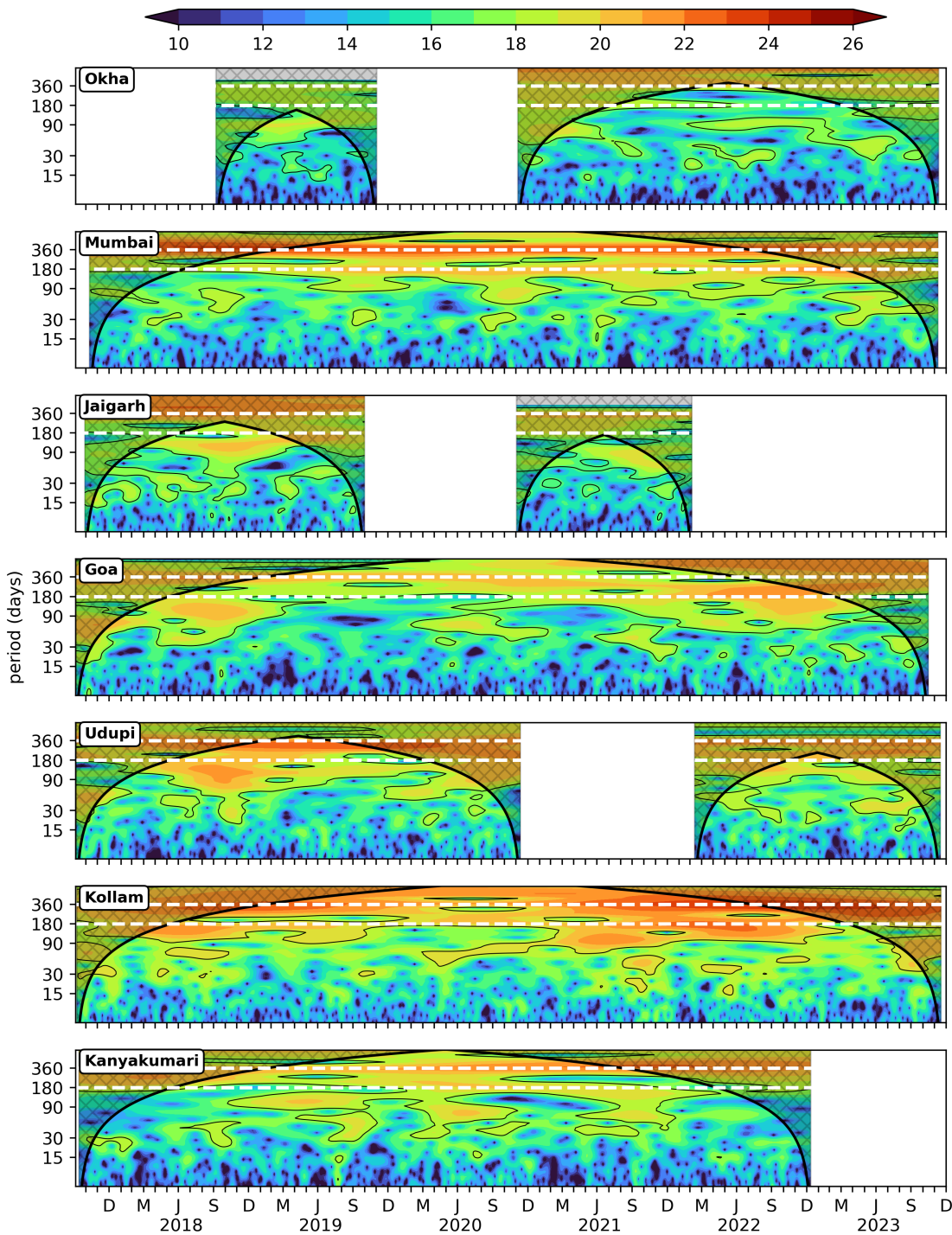


Figure 6: Wavelet power spectra (Morlet) of the 40 m zooplankton biomass plotted against time as abscissa and period in days as ordinate. The wavelet power is in log₂ scale, the 95 % significance is marked in black contours; the cross-shaded region falls under cone of influence.

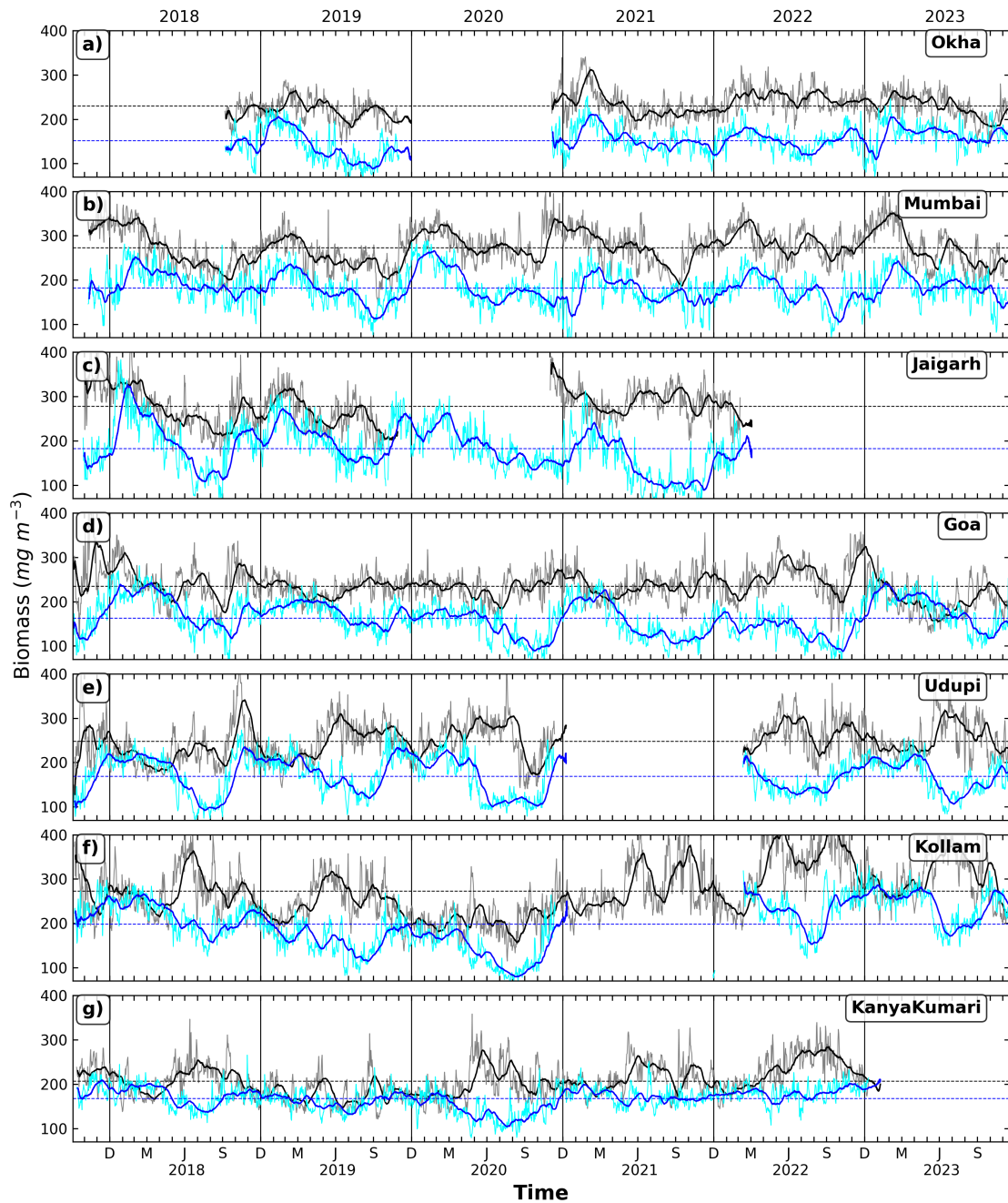


Figure 7: The daily biomass at depth of 40 m and 104 m for all locations shown by grey and cyan curves. The black and blue lines shows the 30 day rolling averaged biomass.